Annals of Biomedical Engineering, Vol. 39, No. 8, August 2011 *(© 2011)* pp. 2263–2273
DOI: 10.1007/s10439-011-0306-5

Assessing Manual Pursuit Tracking in Parkinson's Disease Via Linear Dynamical Systems

MEEKO M. K. OISHI,[1] POURIA TALEBIFARD,[1] and MARTIN J. MCKEOWN[2]

[1]Electrical and Computer Engineering, University of British Columbia, Vancouver, BC, Canada; and [2]Pacific Parkinson's Research Centre, Neurology, and Electrical and Computer Engineering, University of British Columbia, Vancouver, BC, Canada

(Received 6 December 2010; accepted 27 March 2011; published online 6 April 2011)

Associate Editor Nathalie Virag oversaw the review of this article.

Abstract—Quantitative assessment of motor performance is important for diseases of motor control, such as Parkinson's disease (PD). Manual tracking tasks are well suited for motor assessment, as they can be performed concomitantly with brain mapping techniques. Here we propose utilizing second-order linear dynamical systems to assess manual pursuit tracking performance. With the desired trajectory as the input, and the subject's actual motor response as the output, a linear model characterized by natural frequency and damping ratio is identified for each subject. We applied this method to 10 PD subjects (on and off L-dopa medication) and 10 normal subjects performing a multi-frequency sinusoidal tracking task. Model parameters were more sensitive than overall tracking errors in determining significant differences between groups. The effect of L-dopa medication was to reduce the damping ratio and make the range in natural frequency across individuals approach that of normal subjects. We interpret the changes in damping ratio and natural frequency as possibly related to suppression of compensatory cerebellar activity and/or improvement of motor program selection, and the changes in natural frequency as an implicit strategy to maintain settling time in the face of reduce damping ratio. Our results suggest that simple linear dynamical system models can be a powerful method to assess tracking performance in Parkinson's disease because of the additional insight they can provide into neurological processes.

Keywords—Parkinson's disease, Manual tracking, L-Dopa, System identification, LTI systems.

INTRODUCTION

The objective assessment of motor performance is critical for diagnosis of disease states, assessing disease progression, and determining the effects of therapy and rehabilitation. One such condition where motor performance monitoring is important is in Parkinson's disease (PD), the second most common neurodegenerative disease after Alzheimer's.

PD is characterized by tremor, rigidity, bradykinesia (slowness of movement), and postural instability. The characteristic symptoms of PD are mainly the result of premature degeneration in the basal ganglia, a group of structures at the base of the forebrain. While the exact purpose of the basal ganglia has yet to be elucidated, most models of the basal ganglia emphasize the importance of movement selection,[6] and the basal ganglia are most active when a subject must perform an action that is internally guided (e.g., recalled from memory) from many potential candidates of action.[36] Other types of movement, such as externally guided ones, require a subject to move in response to an external stimulus, such as mimicking an action. Externally guided actions are normally associated with activity in the cerebellum where sensorimotor integration is important.[18] The cerebellum, a structure in the hindbrain, traditionally associated with pure motor control, is now considered to be essential for the development of forward models, such as predicting the sensory consequences of motor actions.[26] However, a number of studies have suggested that increased cerebellar activity may partially compensate for deficient basal ganglia circuits (e.g., [29–31]), resulting in alterations in a broad repertoire of movement in PD.

Manual tracking tasks, externally guided movements whereby subjects are asked to track a target or moving object with a hand, or a cursor under manual control, are an increasingly popular means to assess motor performance, as they are conducive to execution during brain mapping procedures (e.g., functional

Address correspondence to Meeko M. K. Oishi, Electrical and Computer Engineering, University of British Columbia, Vancouver, BC, Canada. Electronic mail: moishi@ece.ubc.ca

magnetic resonance imaging (fMRI), electroencephalography (EEG), and positron emission tomography (PET)) where excessive head motion must be prevented. A variety of manual pursuit tracking tasks have been used to characterize PD[20,35] by distinguishing performance measures between PD and normal subjects. Pursuit tracking tasks involve multiple brain functions, including planning, execution, motor control, sensory feedback, and saccadic and smooth pursuit eye movements, so it is difficult to discern with certainty the particular structures of the brain involved in a given task. However, recent research has used manual pursuit tracking to discern the roles of the cerebellum and the basal ganglia, by introducing visual errors in the cursor position,[5,21] tactile changes in the input device,[16] and by using target trajectories with sudden and unexpected changes.[10] In Lemieux *et al.*,[20] an increased response to visual error in dyskinetic movements in PD was attributed to basal ganglia, as opposed to cerebellar, lesions, although the possible role of compensatory cerebellar changes was neglected.

For the experiment described in this paper, we focus on manual pursuit tracking tasks to investigate the potential role of compensatory mechanisms in PD. Essentially, we aim to discern from tracking data the differences in how PD and control subjects accomplish sinusoidal tracking tasks. We postulate that linear dynamical systems are ideally suited to provide insight into qualities of tracking performance that are inherently dynamic, such as slowness and overshooting clinically associated with PD off and on medication, respectively.[16,21,39] We build on our prior work,[5] in which damping ratio and natural frequency, two independent parameters that characterize overshooting and slowness in second-order linear time-invariant dynamical systems, were found to be significantly different between PD and control subjects, and between tracking tasks, respectively.

Other researchers have also investigated linear dynamical system models of manual tracking tasks. Prior work by Abdel-Malek *et al.*[1,2] used discrete-time ARMA models (one formulation of a linear dynamical system) to characterize response to sinusoidal trajectories. For complex tracking tasks involving five harmonically related frequencies, resultant linear dynamical system models varied with different the tracking tasks[13] in a small sample ($N = 5$) of control subjects. While the bandwidth of the tracking trajectory may affect the spectrum over which the model is valid,[3] in PD subjects, the phenomenon of bradykinesia, or slowness of movement, practically restricts sinusoidal tracking to <1 Hz. In related work,[13,32] discrete-time low pass filters (yet another formulation of linear dynamical systems) were used to adaptively filter tremor in PD, which can also be detected with spectral analysis.[4] Lastly, some work has also been done on adaptive and nonlinear models with feedforward components.[9,35]

In contrast to the aforementioned dynamical models, other common measures of tracking performance in PD include root mean square (RMS) error, absolute mean error, maximum error, lag time, peak velocity, and mean velocity.[3,11,17,21,25,38] However, in our previous work as well as in the experiment described in this paper, RMS error, the most common tracking performance metric, appears to be relatively insensitive to the tracking performance in PD, as PD subjects may employ differing implicit strategies compared to normal controls to maintain overall tracking performance. Essentially, RMS error did not convey subtleties of how tracking performance was achieved, despite clear differences evident even upon visual inspection of the data (Fig. 3). Moreover, RMS error ignores the temporal dynamics that may have diagnostic and discriminatory importance. Hence we focus in this paper again on dynamic measures of damping ratio and natural frequency, which provide a measurable interpretation of overshoot and slowness associated with PD.

We suggest that modeling tracking performance with linear dynamical systems, and then using the parameters of the fitted models as features, provides a powerful method for assessing tracking performance. As neuroscientists attempt to elucidate the function of different neural structures during motor tasks, it is natural to consider dynamical systems to provide a theoretical framework for interpreting these studies as these models may incorporate concepts of feedback, model selection, and forward (predictive) models.

METHODS

Tasks

The tracking data were obtained from a simultaneously performed fMRI experiment sanctioned by the University of British Columbia's Ethics Board and fully described elsewhere.[31] In brief, 10 volunteers with clinically diagnosed, mild to moderate PD (Hoehn and Yahr stage 2–3, four men and six women, mean age 66.0 $\pm$ 8 years) and 10 healthy, age-matched subjects without active neurological disorders (three men, seven women, mean age 57.4 $\pm$ 14 years) were recruited for this study. While some subjects may have experienced L-dopa-induced dyskinesias and tremor, these were, by necessity, sufficiently mild so as not to induce excessive movement artifact in the MRI scanner. After obtaining informed consent, subjects viewed a computer screen

via a projection–mirror system while lying in the magnetic resonance scanner. In their right hand, they held a rubber squeeze bulb, which was connected via low-compliance water-filled tubing to a pressure transducer outside the scanner room.

Subjects performed a visually guided tracking task in which they were required to control the width of a black horizontal bar on the screen using the squeeze bulb to keep it within a sinusoidally vertically scrolling pathway (Fig. 1). The width of the bar could be increased by applying greater pressure to the bulb, while releasing pressure from the bulb decreased the width of the bar. The experiment was designed so that subjects were asked to squeeze between 5 and 15% of their maximum voluntary contraction (MVC), so that they could perform the task for extended periods. Subjects performed sinusoidal squeezing tasks in 20 s blocks at three different frequencies (0.25, 0.50, and 0.75 Hz) interspersed with 20 s sections where the target force needed to be constant at 10% MVC. The frequencies of the sinusoidal sections were presented pseudo-randomly. An entire experiment consisted of two blocks of each frequency with interspersed constant contraction, totaling 4 min for six tasks. All subjects performed the 4-min experiment once with the right hand and once with the left hand. To prevent the effects of hand dominance on the tracking results, we restricted the analysis to the data from the right hand only.

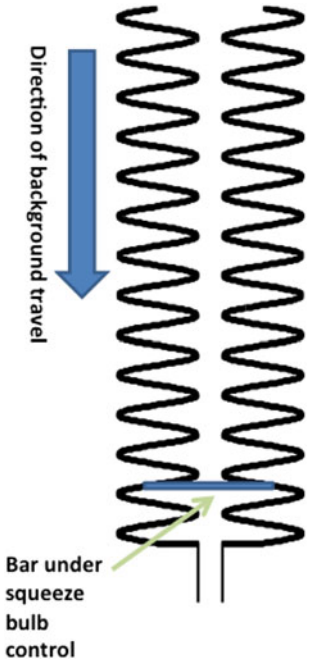

FIGURE 1. Task performed by subjects. Squeezing a pressure bulb increased the size of bar, while releasing pressure reduced the size of the bar. Subjects were instructed to keep the bar within the sinusoidal track as it was scrolling downwards.

PD subjects performed the experiments once after an overnight withdrawal (minimum of 12 h since their last dose of L-dopa, minimum of 18 h since the last dose of dopamine agonists) of their anti-Parkinson drugs and again 1 h after taking L-dopa. All subjects practiced the task at each frequency during a training session (PD subjects completed the training session pre-medication) until errors stabilized and they were familiar with the task requirements. As squeezing is a simple task associated with normal day-to-day usage (as opposed to say, a novel task of reaching within a robot-induced force field,[33] the training period did not emphasize learning a new task, but ensured that subjects were familiar with the setup and comfortable manipulating the squeeze bulb. The first scanning session did not begin until the subject's performance stabilized to this point.

Stimuli were designed and presented using custom Matlab software (Mathworks) and the Psychtoolbox.[7] Matlab was also used to collect behavioral data from the response device with a sampling interval of 0.03 s.

System Identification

Time-series analysis attempts to create a model that fits a known set of input/output data as closely as possible, by minimizing the discrepancy between the output predicted by the model and the actual output data. A variety of time-series modeling frameworks exist, including Box–Jenkins, AR, ARMA, ARMAX, state-space, gray-box, as well as many nonlinear techniques. A variety of computational algorithms to identify time-series models for a given set of input/output data are available in Matlab's System Identification Toolbox (Mathworks, Inc).[22] These models and algorithms are widely used in engineered systems when first principles do not adequately predict realistic system behavior. Building on previous work[2] that established second-order ARMA models as effective in describing sinusoidal tracking performance in PD, we identify models in state-space form, conducive to interpretation of damping ratio and natural frequency as measures of overshoot and slowness in tracking performance. In addition, we note that any dependence in our models with respect to the spectrum of the tracking trajectory is essentially normalized, since the same tracking frequencies are used for all subjects. Hence we assume that the underlying process can be effectively modeled as a linear dynamical system, invariant over the duration of each experiment block.

As per standard system identification techniques,[23] we separate the six blocks of input and output data for the right hand into two sets of three blocks each: one

set for model creation, and one set for model validation. Data from the first set of blocks at three different frequencies were used to create the model, and data from the second set of three blocks were used to validate the model. For each block, we assume the target is the input, and the cursor is the output (denoted input $\rightarrow$ output). System identification algorithms typically minimize the difference between the actual and predicted output for a single block. However, numerical issues arising from the limited frequency content in the input prevented model creation over single frequency target $\rightarrow$ cursor blocks. Minimization of a sum of three weighted differences (one corresponding to each of three target $\rightarrow$ cursor blocks) results in the creation of a single model from three blocks, via Matlab's "merge" function. Hence a single second-order linear dynamical model is created for each subject using optimization-based algorithms for second-order state-space systems in canonical form.

Model Validation

Model validation can be accomplished through a variety of complementary approaches. We first calculated a "fitness score", by estimating the percentage of the output explained by the model. The fitness score depends on the difference between the actual output y and modeled output $\hat{y}$, normalized by the variations in the output from its mean value $\bar{y}$, and was numerically evaluated with Matlab's "compare" function.

$$\text{Fitness score (in \%)} = \left(1 - \frac{\sqrt{\frac{1}{N}\sum_{i=1}^{N}(y[i]-\hat{y}[i])^2}}{\sqrt{\frac{1}{N}\sum_{i=1}^{N}(y[i]-\bar{y})^2}} \right) \times 100$$

After identifying model parameters based on one set of input/output data, an input from another set of input/output is applied to the model to create a modeled output. This output is then compared to the output of the second input/output data set. The fitness score provides an overall measure of how "good" a fit the model provides to the actual data. We validate through a second set of data in accordance with standard system identification techniques,[3] since it indicates how well the model matches independent data that it was not created from, and will therefore be robust to over-fitting.

In contrast, other measures of model assessment (such as loss functions like the Akaike information criterion) indicate how well a model fits the data it was constructed from, while penalizing the use of an excessive number of model parameters (to prevent over-fitting). The Akaike information criterion, as well as the final prediction error and other loss functions, are less useful here since the order of the model is predetermined. However, in examining higher order models for a number of the subjects, the Akaike information criterion confirmed the same result as in Gonzalez *et al.*:[13] higher order models did not provide enough relative benefit in model accuracy to overcome the cost of additional model complexity.

We further assessed the accuracy of our models by completing a sensitivity analysis for each model, with a focus on model parameters utilized in the "Results" section. Covariance estimates, obtained by evaluating how different the model would be if alternative output data were used for with the same input data, were assessed for individual model parameters.[38] The blocks corresponding to the validation data set were used to obtain the alternative output data. For the covariance estimates to be valid, the residual must be uncorrelated with itself to ensure whiteness, and uncorrelated with the input to assure independence.[3] Numerically, the whiteness and independence conditions are evaluated to within a 99% confidence interval, that is, to within 2.58 standard deviations.

The identified canonical models take the form

$$\begin{aligned} x[k+1] &= \begin{bmatrix} 0 & 1 \\ \hat{a}_1 & \hat{a}_0 \end{bmatrix} x[k] + \hat{B}u[k] \\ \hat{y}[k] &= [\,1 \quad 0\,]x[k] + \hat{D}u[k] \end{aligned} \tag{1}$$

with the difference between actual output and modeled output $y[k] - \hat{y}[k] = w[k]$ modeled as a white noise process with zero mean and variance Q. The matrices $\hat{B} \in \Re^{2\times 1}$, $\hat{D} \in \Re$ and scalar values $\hat{a}_0$, $\hat{a}_1$, Q, are constant. Hence the system identification calculates a total of six unknown model parameters (chosen to minimize Q),[38] and the noise process represents the portion of the output that the model could not account for.

Analysis of Linear Dynamical Systems

With such a high sampling rate, the resultant model can be more intuitively rewritten as a continuous-time second-order linear dynamical system by using a zero-order hold transformation.[12]

Consider a generic continuous-time second-order linear dynamical system model,

$$\begin{aligned} \frac{d}{dt}x(t) &= Ax(t) + Bu(t) \\ \hat{y}(t) &= Cx(t) + Du(t) \end{aligned} \tag{2}$$

for which the input $u(t)$ represents the target position at time t, and the output $y(t) = \hat{y}(t) + w(t)$ that represents the cursor position at time t is the sum of the modeled output and a white noise process $w(t)$. The signal $w(t)$ is the value at time t of an independent and

identically distributed Gaussian process with covariance Q that the model cannot capture. (Note that for the conversion from discrete-time to continuous-time, $u(0.03{\cdot}i) = u[i]$, $y(0.03{\cdot}i) = y[i]$, $w(0.03{\cdot}i) = w[i]$.) The state $x(t)$ is a representation of the internal status of the system at time t, and is not directly measurable. For a two-dimensional system, $x(t)$ is a time-varying vector with two elements. The first and second elements of the state are the cursor position and velocity, respectively. The matrices $A \in \Re^{2\times2}$, $B \in \Re^{2\times1}$, $C \in \Re^{1\times2}$, $D \in \Re$ are constant.

Since for dynamics given by Eq. (2) the predicted output is

$$\hat{y}(t) = Ce^{At}x(0) + \int_0^t e^{A(t-\tau)}Bu(\tau)d\tau \tag{3}$$

we analyze the eigenvalues $\lambda_{1,2}$ of A in Eq. (1). The eigenvalues characterize performance in both transient and steady-state responses, and satisfy the second-order characteristic equation

$$\begin{aligned} 0 &= |\lambda I - A| \\ &= \lambda^2 + a_1\lambda + a_0 \end{aligned}$$

for some positive real numbers a_0, a_1. Rewritten in terms of performance parameters ζ, $\omega_n > 0$,

$$0 = \lambda^2 + 2\zeta\omega_n\lambda + \omega_n^2, \tag{4}$$

the characteristic equation determines the behavior of the models. That is, parameters ζ and ω_n provide intrinsic measures of what makes the modeled dynamics unique.

The matrices A, B, C, D completely characterize all possible system responses, that is, once tracking performance is successfully modeled, then the output y can in theory be predicted for any given input u, not just those that were chosen experimentally. The solution to (1) will follow trajectories determined by model parameters ζ, ω_n, input trajectory u, and known initial state $x(0)$. Additionally, the state x, though not measurable directly, can be reconstructed from a known initial condition and a known input sequence.

To illustrate, consider the response of such a system to a Heaviside function (a step input), as in Fig. 2a. The natural frequency describes the frequency of oscillations intrinsic to the model (irrespective of the frequency that the system is stimulated at), while the damping ratio describes the amount of "undershoot"

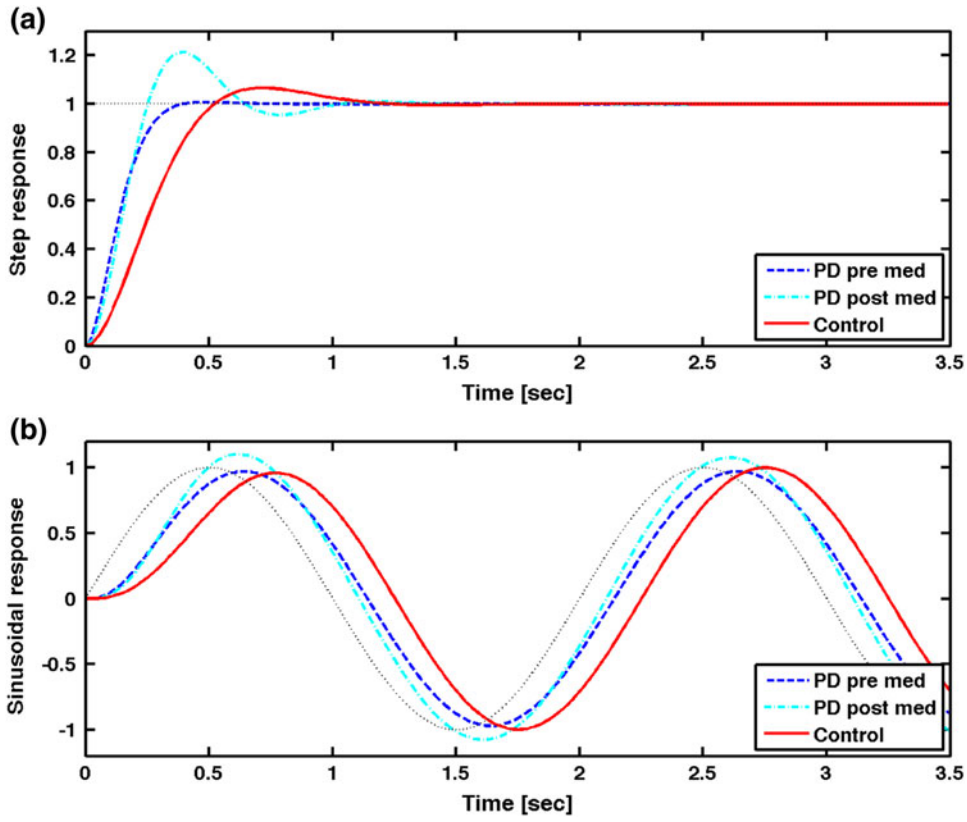

FIGURE 2. Typical results based on mean value parameters for the response to (a) a Heaviside function, and (b) a sinusoidal function, for each of the three groups studied. The damping ratio and natural frequency have the same qualitative effect in both (a) and (b), although in practice, the validity of our models may not extend to functions (such as in (a)) with high frequency content.

or "overshoot" in the response. For $\zeta < 1$, Eq. (3) describes an underdamped response that oscillates in a decaying fashion in response to a step input. For $\zeta > 1$, Eq. (3) describes an overdamped response that converges without oscillation. The product of the two parameters, $\zeta\omega_n$, describes the rate of decay of oscillations and is known as the decay rate. This quantity is inversely proportional to the settling time $T_s \approx 4/(\zeta\omega_n)$, which is the amount of time required for the output response to a unit step input to subside to within 0.01 of the final value.

Similar transient behaviors will occur in response to other input signals, including sinusoidal inputs such as those used in this experiment (Fig. 2b). In addition, frequency response characteristics such as gain and phase can also be used to describe the steady-state response of (2) to a sinusoidal input at an arbitrary frequency. The relative gain and phase shift of the output $y(t)$ with respect to an input $u(t) = \sin(\omega t)$ will vary depending on the relative value of the input frequency ω with respect to the natural frequency ω_n, as well as the damping ζ inherent to the system. We use the more general formulation (3) since it encompasses both transient and steady-state behavior, however, gain and phase lag can easily be calculated once ζ and ω_n are determined.[8]

The main limitation of our model is that, as shown in Sugi *et al.*,[35] in practice such models are only valid for input signals whose frequency content is near to those frequencies used in model creation. This is not a severe limitation, however, as the range of frequencies over which one can rapidly squeeze a bulb is fairly limited. Hence while Fig. 2a provides the most intuitive description of damping ratio and natural frequency, the high frequency content of a step input likely exceeds those frequencies over which our model is valid. The subtle differences between groups in Fig. 2b is a more accurate representation of the differences our model can accommodate.

RESULTS

We performed ANOVA tests across three groups (PD pre, PD post, Controls) and paired t tests for PD subjects only (PD pre, PD post). While the ANOVA tests may decrease the statistical power of the groups PD pre, PD post, the presence of the Control group requires the use of ANOVA tests for unpaired measures. Results are summarized in Table 1.

The RMS error, calculated as

$$E_{\mathrm{RMS}} = \sqrt{\frac{1}{N}\sum_{i=1}^{N}(y[i] - u[i])^2}$$

with $u[i]$ the desired position at time index i, $y[i]$ the actual tracking done by the individual at time index i, and N the total number of time points, was not significant across groups using ANOVA ($p = 0.2109$) or in a paired t test between PD subjects off medication ("PD pre") and Parkinson's subjects on medication ("PD post") ($p = 0.3109$).

The model fitness scores were $72.2 \pm 5.3\%$ for normal subjects, $65.9 \pm 12.0\%$ for Parkinson's subjects off medication, and $69.6 \pm 11.3\%$ for Parkinson's subjects on medication. These scores indicate relatively good fits between the model and the data.

The covariance of $(\hat{a}_0\ \hat{a}_1)$ had a mean value of $(0.0255 \pm 0.0057,\ 0.0265 \pm 0.0067)$ for normal subjects, $(0.0314 \pm 0.0093,\ 0.0327 \pm 0.0105)$ for PD pre, and $(0.0220 \pm 0.0025,\ 0.0228 \pm 0.0228)$ for PD post—all values are an order of magnitude smaller than $(\hat{a}_0\ \hat{a}_1)$. All models but one passed at least one independence test; all but two models passed at least one whiteness test. The one model that did not pass the independence test (PD pre) fell within a confidence interval of 99.9%, and had a high fitness score (74.40%). The two models that did not pass the whiteness tests (both PD pre) were just outside of the confidence intervals, with values corresponding to

TABLE 1. Summary of statistical tests for damping ratio, natural frequency, decay rate, rise time, and RMS error across groups.

	PD pre	PD post	Normal	Statistical tests
Damping ratio ζ	0.75 ± 0.23	0.47 ± 0.19	0.67 ± 0.24	Paired t test, $p = 0.0046$ ANOVA, $p = 0.0249$
Natural frequency ω_n (rad/s)	8.34 ± 2.60	7.60 ± 1.85	7.00 ± 1.11	Paired t test, $p = 0.2500$ ANOVA, $p = 0.3205$ Variance, $p = 0.0610$
Decay rate $\zeta\omega_n$ (rad/s)	6.33 ± 2.84	3.35 ± 1.12	4.67 ± 1.88	Paired t test, $p = 0.0063$ ANOVA, $p = 0.0122$
Settling time T_s (s)	0.77 ± 0.35	1.47 ± 1.02	0.99 ± 0.41	Paired t test, $p = 0.0674$ ANOVA, $p = 0.0748$
RMS error E_{RMS} (mm)	81.42 ± 21.81	72.70 ± 21.42	68.16 ± 11.57	Paired t test, $p = 0.2322$ ANOVA, $p = 0.3109$

99.7% and 99.2% levels, but also had relatively high fitness scores (71.49% and 64.60%). No model failed both independence and whiteness tests. In addition, upon visual inspection, all models that failed either the independence or whiteness tests still appeared to maintain good representations of input–output behavior.

Frequency response characteristics gain and phase lag were not significant across groups for any of the three input frequencies ($p = 0.0927, p = 0.1632$, respectively, for 0.25 Hz; $p = 0.0617$, $p = 0.2407$, respectively, for 0.5 Hz; $p = 0.0685, p = 0.4253$, respectively, for 0.75 Hz).

Typical responses to a Heaviside function, and to a sinusoidal function, are shown in Figs. 2a and 2b, respectively, using mean values of ζ, ω_n for each group. Figure 3 demonstrates the input, output, and modeled output for a typical PD subject, pre- and post-medication, and a typical normal subject.

For normal subjects, the damping ratio had a mean value of 0.67 ± 0.24, while for Parkinson's subjects off medication it was 0.75 ± 0.23, and for Parkinson's subjects on medication it was 0.47 ± 0.19. The differences in mean damping ratio were significant across all groups ($p = 0.0046$ ANOVA) and when a paired t test was performed on the PD subjects on/off medication, the result was also significant ($p = 0.0249$ paired t test, Fig. 4).

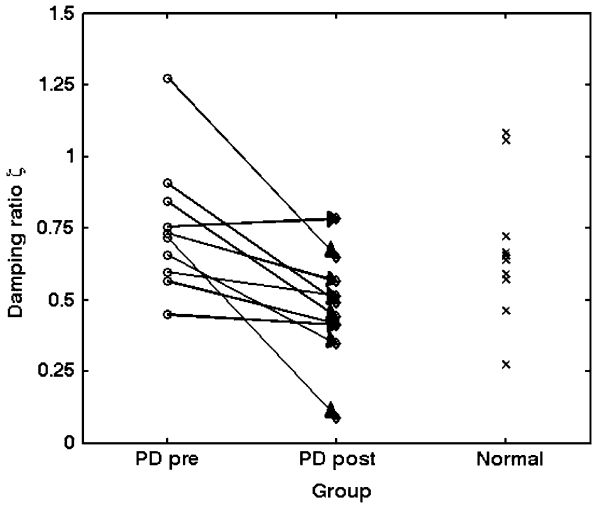

FIGURE 4. Changes in damping ratio. The arrows are drawn so that the effects of L-dopa medication can be seen: the head and tail of each arrow represent the same PD subject. Note the downward trend in all but one arrow, indicating that the main effect of L-dopa medication is reduction of damping ratio.

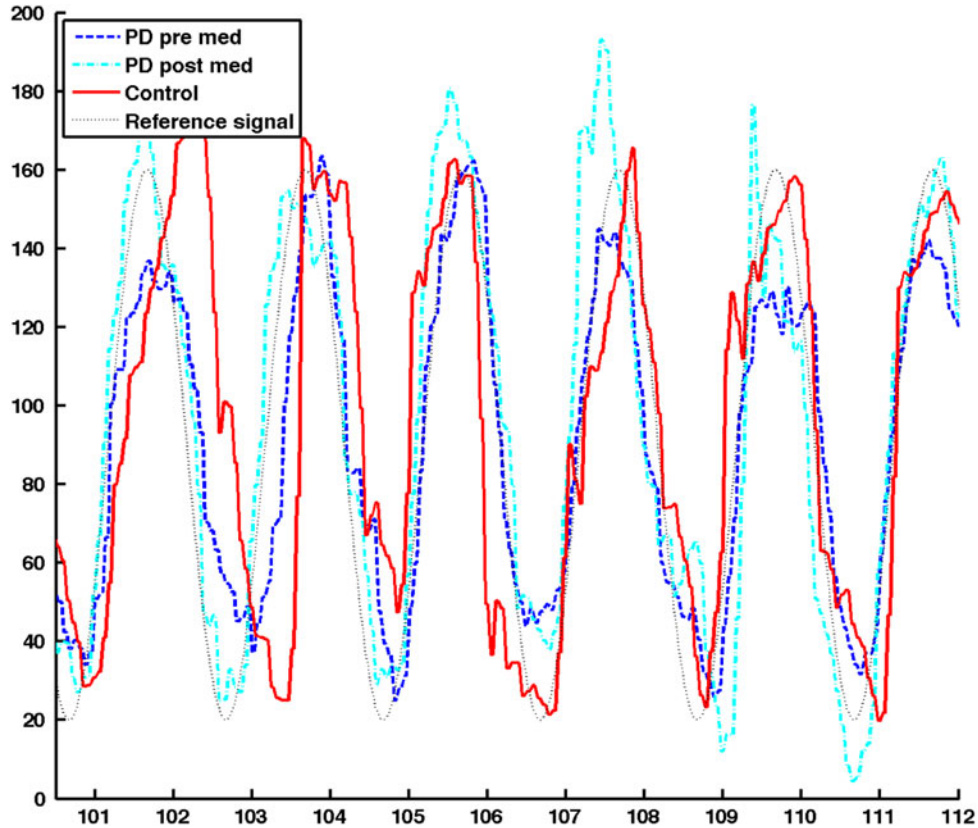

FIGURE 3. A comparison of input, actual output, and modeled output for part of the sinusoidal task for a typical PD subject, both off and on medication, and a typical Control subject.

The mean natural frequency for normal subjects was 7.00 ± 1.11. For Parkinson's subjects off medication, the mean natural frequency was 8.34 ± 2.60, while for Parkinson's subjects on medication, the mean natural frequency was 7.60 ± 1.85. The means of the natural frequency were not significantly different across groups ($p = 0.3205$ ANOVA), or between PD subjects pre/post-medication in a paired t test ($p = 0.2500$). However, the variance in natural frequency approached significance across groups ($p = 0.0610$, variance test, Fig. 5).

There was no significant correlation between the RMS error and damping ratio for PD pre ($p = 0.1672$) or normal subjects ($p = 0.4661$), but significance for PD post ($p = 0.0448$), with correlation coefficient −0.6778. There was no significant correlation between RMS error and natural frequency ($p = 0.3499$ PD pre, $p = 0.3694$ PD post, $p = 0.1899$ normal). The relationship between RMS error and damping ratio is shown in Fig. 6.

The normality of distributions of natural frequency and damping ratio for each group was evaluated with the Lilliefors test. In all cases (PD pre, PD post, normal), both damping ratio ($p = 0.3883$ PD pre, $p > 0.50$ PD post, and $p = 0.1938$ normal) and natural frequency ($p = 0.4371$ PD pre, $p = 0.4395$ PD post, and $p = 0.1737$ normal) did not appear to come from a non-normal distribution. Similarly, the change in damping ratio for Parkinson's subjects after medication also did not fail the Lilliefors test ($p = 0.4518$). The change in natural frequency for Parkinson's subjects pre/post-medication did not fail the Lilliefors test, either ($p > 0.50$). We additionally performed a non-parametric statistical test, the Wilcoxon signed rank test, on the change in damping ratio ($p = 0.0039$) and on the change in natural frequency ($p = 0.3223$) pre/post-medication. Hence the result in damping ratio (Fig. 4) is significant. The result for natural frequency may arise from a non-normal distribution. We also evaluated common transformations of natural frequency ($\log \omega_n$, $\sqrt{\omega_n}$, $1/\sqrt{\omega_n}$, $1/\omega_n$) across groups, but did not obtain any additional significance ($p = 0.4563$, $p = 0.3838$, $p = 0.5357$, $p = 0.6184$, respectively).

Lastly, while settling time showed no significance across groups ($p = 0.0748$ ANOVA) decay rate was significant across groups ($p = 0.0122$ ANOVA). For normal subjects, the decay rate was 4.67 ± 1.88 rad/s, while for Parkinson's subjects off medication, it was 6.33 ± 2.84 s, and for Parkinson's subjects on medication it was 3.35 ± 1.12 s. A paired t test performed on PD subjects on/off medication yielded a significant result ($p = 0.0063$, paired t test). There was no significant correlation between RMS error and decay rate for normal ($p = 0.1762$) or PD pre-subjects ($p = 0.1371$), but significant correlation does exist for PD post-subjects ($p = 0.0273$). No significant correlation between RMS error and settling time exists for any group ($p = 0.3027$ normal, $p = 0.1387$ PD pre, $p = 0.0593$ PD post).

To further ensure the robustness of the statistical differences we observed, we employed the method of surrogates.[34] One thousand surrogate models were created for each subject, by randomly choosing $(\hat{a}_0\ \hat{a}_1)$ from Eq. (1) according to their Gaussian distributions. Damping ratio, natural frequency, decay rate, and settling time were computed for each of the 1000 models per subject. To validate the t test results in Table 1, we randomly chose one model (out of 1000

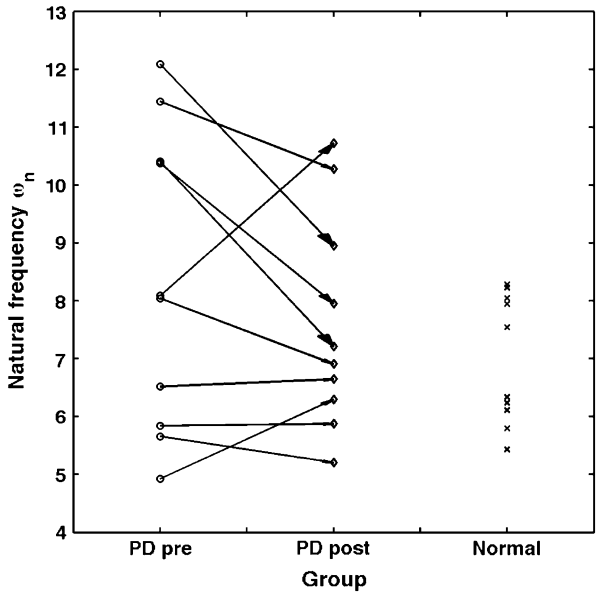

FIGURE 5. Changes in natural frequency. As in Fig. 4, each arrow corresponds to a different PD subject. Note the reduction in inter-subject variability after L-dopa medication.

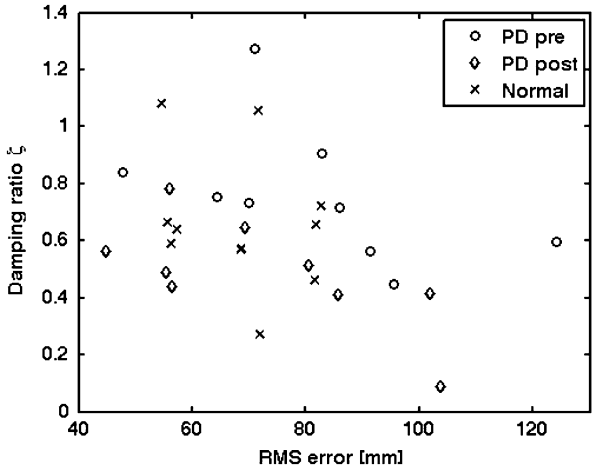

FIGURE 6. Scatterplot of RMS error and damping ratio for all subjects.

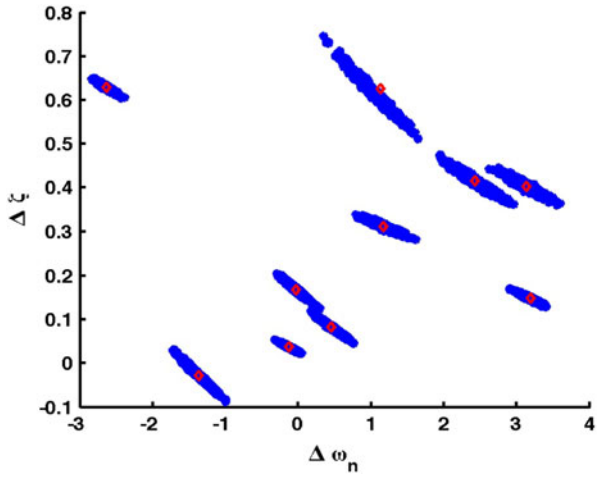

FIGURE 7. From models created from surrogate data, the change in damping ratio and change in natural frequency for each subject, before and after medication. Notice that for all but one subject, the damping ratio decreases after medication ($\Delta\zeta = \zeta_{PDpost} - \zeta_{PDpre} > 0$). The product of the damping ratio and natural frequency (the decay rate) is also statistically significant before and after medication.

possible models) for each subject, randomly permuted all labels (PD pre or PD post), then computed the standard t-test measure of the difference in means, that is, E(PD pre) − E(PD post) for the parameter of interest. We repeated this process 1000 times, to obtain new values $p = 0.0200$ for damping ratio ζ, $p = 0.2230$ for natural frequency ω_n, $p = 0.0200$ for decay rate $\zeta\omega_n$, and $p = 0.2630$ for settling time T_s, respectively. The surrogate values for the difference in ζ, ω_n before and after medication for all PD subjects are shown in Fig. 7. This additional step precludes potential issues of non-whiteness due to small sample size and variability in model parameters for damping ratio ζ and decay rate $\zeta\omega_n$.

DISCUSSION

The dynamical models identified here provide unique insight into motor performance in PD over and above the standard metric of RMS error, as RMS error did not reveal significant differences between normal subjects and PD subjects on and off medication. Furthermore, the lack of correlation between RMS error and natural frequency for all groups, and between RMS error and damping ratio for normal and PD_pre-medication groups (Fig. 6), suggests that additional, independent information is provided by the model parameters. L-Dopa medication significantly reduced the damping ratio after medication (Fig. 4). Moreover, medication appeared to reduce the already-increased[39] intersubject variability in natural frequency seen in PD subjects off medication, so that post-medication, the range was more like that of control subjects (Fig. 5). While overlap between groups impedes discrimination of individual subjects, trends across groups are noticeable and statistically significant.

Surprisingly, gain and phase lag did not provide insight to the observed performance (as in, e.g., Flowers[11]), while damping ratio and natural frequency did. Since gain and phase lag can be expressed as a nonlinear transformation of damping ratio and natural frequency, one potential explanation is the potential non-normality of the gain and phase lag distributions after transformation that may affect standard tests that assume a normal distribution. We additionally note that there is a non-unique mapping from gain to input frequency for most second-order transfer functions, especially in the frequencies near or below the natural frequency, making significance between groups difficult to detect.

Damping ratio and natural frequency both have fairly intuitive interpretations for observed tracking performance. It is perhaps surprising that these parameters, based on a black-box approach encompassing complex interactions between visual and motor mental functions, can indicate significantly different manual tracking performance between PD and normal subjects. A damping ratio of <1, i.e., an underdamped linear dynamical system response, corresponds to tracking performance that overshoots and oscillates around a desired target, as empirically observed in many of the PD subjects after medication (Fig. 3). A damping ratio >1, i.e., an overdamped linear dynamical system response, corresponds to tracking performance that undershoots and may never quite reach the desired target, effectively shortcutting difficult-to-reach peaks. Natural frequency represents the speed of system-specific oscillations that are independent of the particular input signal applied. For the tracking data presented here, the natural frequency ω_n represents the tendency of the modeled output to oscillate as the subject attempts to track a moving target. Lastly, decay rate $\zeta\omega_n$ provides a measure of how quickly a desired change in the cursor trajectory is accomplished.

We have taken precautions to ensure that possible changes in motor learning rates are not a plausible explanation for the differences in observed motor performance. When a subject is presented with a new motor task, the subject usually experiences an initial rapid decrease in movement related errors related to explicit (conscious/intentional) learning. Much slower decreases in errors are related to implicit (unconscious/incidental) learning.[15,34] In our study, all subjects, both PD and controls, completed a training session until errors asymptotically converged. In addition, our task

is sufficiently simple and overlearned (i.e., practiced beyond the initial point of mastery) because squeezing is used in day-to-day tasks, that we assume explicit learning is not an issue. Thus we assert that the difference in strategies relates to the result of implicit learning of the overlearned task that has occurred over the duration of illness.

Our results are consistent with recent interpretations about motor performance in PD. The differences in damping ratio, particularly after PD subjects received L-dopa medication, may be related to changes in cerebellar compensatory activation, as subjects with cerebellar damage have underdamped movements.[24] While many other factors can affect tracking, using subjects as their own internal control and directly comparing model parameters pre/post-medication on a subject-by-subject basis (e.g., Fig. 4) will tend to minimize these effects. As there is evidence of cerebellar hyperactivation in PD, presumably as a macroscopic compensation for the diseased BG,[40] we interpret our results as being suggestive of L-dopa-induced reversal of compensatory overactive cerebellar activity. Another possibility is that activity in the indirect pathway of the basal ganglia, which is excessive in PD, may result in selection of antagonistic motor programs resulting in co-contraction and increased damping ratio.[19] L-Dopa may partially normalize this abnormal motor selection deficit, and thus reduce overall damping ratio. We note that normalization of both basal ganglia and cerebellar activity are not mutually exclusive, and are compatible with recent work demonstrating connections between these two motor subsystems.[14]

Our results demonstrate that PD subjects off medication have a large range in natural frequency (Fig. 5), with some subjects having very large natural frequencies (above the maximum seen in controls subjects of approximately 8.5 rad/s). There are several possible explanations for this variability. One possibility is that it reflects an inability to select amongst competing motor programs, the purported normal role of the BG.[27] If an incorrect motor program is chosen, a wide range of behaviors could be exhibited, resulting in an increase in intersubject variability in natural frequency that we observed (Fig. 5). Higher natural frequencies may be indicative of an implicit strategy of co-contraction of agonist/antagonist muscles that has been previously demonstrated in Parkinson's disease,[28] and has been shown to be associated with an increase in movement frequency.[37] Given the propensity of PD subjects to have lower damping ratios, the increase in natural frequency may be a compensatory mechanism to maintain as high a decay rate ($=\zeta\omega_n$), and hence as short a settling time ($\approx 4/\zeta\omega_n$) as possible. However, this strategy comes at a price: in addition to a potentially increased sensitivity to noise, co-contraction can be fatiguing. While the experiment was, out of necessity, designed to occur in a frequency range in which PD subjects can successfully track sinusoidal movements, this compensatory mechanism would be less suitable for a broader repertoire of movements (e.g., those at higher frequencies).

CONCLUSION

We propose that the parameters of fitted second-order linear dynamical system models provide a sensitive and informative way to monitor manual tracking performance in Parkinson's disease.

ACKNOWLEDGMENTS

The authors are grateful to Samantha Palmer for assistance in collecting the data. This work was supported in part by a Michael Smith Foundation for Health Research Team Startup Grant (McKeown), by NSERC Discovery Grant #327387 (Oishi), and by an NSERC USRA (TalebiFard).

REFERENCES

[1]Abdel-Malek, A., C. Markham, P. Marmarelis, and V. Marmarelis. Quantifying deficiencies associated with Parkinson's disease by use of time-series analysis. *Electroencephalogr. Clin. Neurophysiol.* 69(1):24, 1988.

[2]Abdel-Malek, A., and V. Z. Marmarelis. Modeling of task-dependent characteristics of human operator dynamics pursuit manual tracking. *IEEE Trans. Syst. Man Cybern.* 18(1):163–172, 1988.

[3]Allen, D. P., J. R. Playfer, N. M. Aly, P. Duffey, A. Heald, S. L. Smith, and D. M. Halliday. On the use of low-cost computer peripherals for the assessment of motor dysfunction in Parkinson's disease—Quantification of bradykinesia using target tracking tasks. *IEEE Trans. Neural Syst. Rehabil. Eng.* 15(2):286–294, 2007.

[4]Aly, N., J. Playfer, S. Smith, and D. Halliday. A novel computer-based technique for the assessment of tremor in Parkinson's disease. *Age Ageing* 36(4):395–399, 2007.

[5]Au, W.-L., N. Lei, M. M. K. Oishi, and M. J. McKeown. L-dopa induces under-damped visually-guided motor responses in Parkinson's disease. *Exp. Brain Res.* 202(3): 553–559, 2010.

[6]Bar-Gad, I., and H. Bergman. Stepping out of the box: Information processing in the neural networks of the basal ganglia. *Curr. Opin. Neurobiol.* 11(6):689–695, 2001.

[7]Brainard, D. H. The psychophysics toolbox. *Spat. Vis.* 10(4):433–436, 1997.

[8]Brogan, W. Modern Control Theory (3rd ed.). Upper Saddle River, NJ: Prentice Hall, 1991.

[9]Davidson, P., R. Jones, J. Andreae, and H. Sirisena. Simulating closed- and open-loop voluntary movement: a

nonlinear control-systems approach. *IEEE Trans. Biomed. Eng*. 49(11):1242–1252, 2002.
[10]Day, B., J. Dick, and C. Marsden. Patients with Parkinson's disease can employ a predictive motor strategy. *J. Neurol. Neurosurg. Psychiatry* 47(12):1299, 1984.
[11]Flowers, K. Some frequency response characteristics of Parkinsonism on pursuit tracking. *Brain* 101(1):19–34, 1978.
[12]Franklin, G., M. Workman, and D. Powell. Digital Control of Dynamic Systems. Boston, MA, USA: Addison-Wesley Longman Publishing Co., Inc, 1997.
[13]Gonzalez, J., E. Heredia, T. Rahman, K. Barner, and G. Arce. Optimal digital filtering for tremor suppression. *IEEE Trans. Biomed. Eng*. 47(5):664–673, 2000.
[14]Hoshi, E., L. Tremblay, J. Feger, P. L. Carras, and P. L. Strick. The cerebellum communicates with the basal ganglia. *Nat. Neurosci*. 8:1491–1493, 2005.
[15]Hwang, E. J., M. A. Smith, and R. Shadmehr. Dissociable effects of the implicit and explicit memory systems on learning control of reaching. *Exp. Brain Res*. 173(3):425–437, 2006.
[16]Johnson, M. T. V., A. N. Kipnis, J. D. Coltz, A. Gupta, P. Silverstein, F. Zwiebel, and T. Ebner. Effects of levodopa and viscosity on the velocity and accuracy of visually guided tracking in Parkinson's disease. *Brain* 119(3):801–813, 1996.
[17]Jones, R., M. Donaldson, and B. Sharman. A technique for removal of the visuoperceptual its application to Parkinson's disease. *IEEE Trans. Biomed. Eng*. 43(10):1001, 1996.
[18]Jueptner, J., M. Jueptner, I. H. Jenkins, D. J. Brooks, R. S. J. Frackowiak, and R. E. Passingham. The sensory guidance of movement: a comparison of the cerebellum and basal ganglia. *Exp. Brain Res*. 112(3):462–474, 1996.
[19]Kaji, R., R. Urushihara, N. Murase, H. Shimazu, and S. Goto. Abnormal sensory gating in basal ganglia disorders. *J. Neurol*. 252:13–16, 2005.
[20]Lemieux, S., M. Ghassemi, M. Jog, R. Edwards, and C. Duval. The influence of levodopa-induced dyskinesias on manual tracking in patients with Parkinson's disease. *Exp. Brain Res*. 176(3):465–475, 2007.
[21]Liu, X., R. Osterbauer, T. Z. Aziz, R. C. Miall, and J. F. Stein. Increased response to visual feedback of drug-induced dyskinetic movements in advanced Parkinson's disease. *Neurosci. Lett*. 304(1–2):25–28, 2001.
[22]Ljung, L. System Identification Toolbox for Use with Matlab. Natick, MA: The Mathworks. Inc., 1997.
[23]Ljung, L., and E. Ljung. System Identification: Theory for the User. Englewood Cliffs, NJ: Prentice-Hall, 1987.
[24]Manto, M. Mechanisms of human cerebellar dysmetria: experimental evidence and current conceptual bases. *J. Neuroeng. Rehabil*. 6(1):10, 2009.
[25]Mates, J., and T. Radil. Two-dimensional manual tracking of periodic movements: event and time interval analyses. *Int. J. Psychophysiol*. 12(2):123–132, 1992.
[26]Miall, R., D. Weir, D. Wolpert, and J. Stein. Is the cerebellum a Smith predictor? *J. Mot. Behav*. 25(3):203–216, 1993.
[27]Mink, J. The basal ganglia: focused selection and inhibition of competing motor programs. *Prog. Neurobiol*. 50(4):381–425, 1996.
[28]Ohye, C., N. Tsukahara, and H. Narabayashi. Rigidity and disturbance of reciprocal innervation. *Confin. Neurol*. 26:24–40, 1965.
[29]Palmer, S., L. Eigenraam, T. Hoque, R. McCaig, A. Troiano, and M. J. McKeown. Levodopa-sensitive, dynamic changes in effective connectivity during simultaneous movements in Parkinson's disease. *Neuroscience* 158(2):693–704, 2009.
[30]Palmer, S. J., J. Li, Z. J. Wang, and M. J. McKeown. Joint amplitude and connectivity compensatory mechanisms in Parkinson's disease. *Neuroscience* 166(4):1110–1118, 2010.
[31]Palmer, S., B. Ng, R. Abugharbieh, L. Eigenraam, and M. J. McKeown. Motor reserve and novel area recruitment: amplitude and spatial characteristics of compensation in Parkinson's disease. *Eur. J. Neurosci*. 29:2187–2196, 2009.
[32]Riviere, C., and N. Thakor. Modeling and canceling tremor in human-machine interfaces. *IEEE Eng. Med. Biol. Mag*. 15(3):29–36, 1996.
[33]Shadmehr, R., and H. H. Holcomb. Neural correlates of motor memory consolidation. *Science* 277(5327):821–825, 1997.
[34]Smith, M. A., A. Ghazizadeh, and R. Shadmehr. Interacting adaptive processes with different timescales underlie short-term motor learning. *PLoS Biol*. 4(6):e179, 2006.
[35]Sugi, T., M. Nakamura, J. Ide, and H. Shibasaki. Modeling of motor control on manual tracking for developing a handmovement-compensation technique. *Artif. Life Robotics* 7(3):112–117, 2003.
[36]van Donkelaar, P., J. F. Stein, R. E. Passingham, and R. C. Miall. Temporary inactivation in the primate motor thalamus during visually triggered and internally generated limb movements. *J. Neurophysiol*. 83(5):2780–2790, 2000.
[37]Verdaasdonk, B., H. Koopman, and F. van der Helm. Resonance tuning in a neuro-musculo-skeletal model of the forearm. *Biol. Cybern*. 96(2):165–180, 2007.
[38]Watson, R., R. Jones, and N. Sharman. Two-dimensional tracking tasks for quantification of sensory-motor dysfunction and their application to Parkinson's disease. *Med. Biol. Eng. Comput*. 35(2):141–145, 1997.
[39]Wenzelburger, R., B.-R. Zhang, S. Pohel, S. Klebe, D. Lorenz, J. Herzog, H. Wilms, G. Duschl, and P. Krack. Force overflow and levadopa-induced dyskinesias in Parkinson's disease. *Brain* 125:871–879, 2002.
[40]Yu, H., D. Sternad, D. M. Corcos, and D. E. Vaillancourt. Role of hyperactive cerebellum and motor cortex in Parkinson's disease. *Neuroimage* 35(1):222–233, 2007.